



DOI: 10.17512/bozpe.2021.1.16

Construction of optimized energy potential  
Budownictwo o zoptymalizowanym potencjale energetycznym

ISSN 2299-8535 e-ISSN 2544-963X



## A comparative numerical analysis of glued laminated timber beams reinforced with bars made of various materials

Damian Jończyk<sup>1</sup> (*orcid id: 0000-0003-2161-4768*)

<sup>1</sup> Czestochowa University of Technology

**Abstract:** The use of fibrous composites to reinforce various structures is an increasingly common practice in construction. Wooden structures are commonly reinforced with composite materials. However, due to the lack of standard regulations for the design of reinforcements with the use of composites, many structural calculations are made in numerical analysis programs using the Finite Element Method (FEM). The article presents numerical calculations of glued laminated timber beams reinforced with various composite rods made using basalt, aramid, glass and carbon fibers. The stiffnesses and the normal stress distributions of the reinforced beam and the comparative, unreinforced beam were compared. The most effective reinforcement found uses carbon CFRP rods.

**Keywords:** glulam, fiber composites, FRP, FEM, numerical analysis

Access to the content of the article only on the bases of the Creative Commons licence CC BY-NC-ND 4.0

Please, quote this article as follows:

Jończyk D., A comparative numerical analysis of glued laminated timber beams reinforced with bars made of various materials, BoZPE, Vol. 10, No 1/2021, 151-159, DOI: 10.17512/bozpe.2021.1.16

### Introduction

Strengthening wooden structures is a long-used solution, being used to both strengthen existing objects (Nowak et al., 2013) and new elements (Yang et al., 2016). Reinforcements are made in very different forms. The most commonly used reinforcing elements are: tapes, mats and rods (Jończyk, 2019), made of various materials such as steel (Jasieńko & Nowak, 2014) and composites (Raftery & Kelly, 2015). Fibrous composites, reinforced with various fibers: carbon, glass, aramid and basalt, are often used composites for reinforcing wooden elements (Holloway, 2010). Tapes and mats are a relatively well-studied method of reinforcement (Campilho et al., 2010; Kim & Haries, 2010; Lu et al., 2015). In the case of rods, the literature provides information on the positive (Jończyk, 2019) and negative impact of the

applied reinforcement (Fosetti et al., 2015). The differences in the influence of the bars used on the load-bearing capacity and the stiffness are related to the different methods of wood-composite connection. Moreover, there are few studies compiling the results for a particular method of reinforcement, but with the use of different materials.

The aim of the article is to compare the stiffness and the distribution of normal stresses in the cross-section of beams reinforced with the same method, using bars made of various composite materials: aramid, basalt, glass, carbon, using a numerical analysis. The comparison may prove useful in evaluating the most advantageous construction materials for the reinforcement of glued laminated timber beams.

## 1. Materials and methods

Numerical modeling is one of the most effective methods of estimating the static work of structural elements. With the use of FEM, it is possible to carry out analyzes that are difficult or impossible to perform through experimental research. The comparative analysis was performed with the use of numerical FEM calculations. One static diagram of a glued laminated timber beam with one reinforcement diagram in the form of composite bars made of different materials was adopted for the calculations.

### 1.1. Materials

**Timber.** The beams were modeled as wooden from glued laminated timber of GL24h class. Due to the fact that in most cases people designing structural elements rely on design standards, the material data presented in the standard (PN-EN 338: 2016-06), presented in Table 1, were used for the calculation. The constitutive model was taken to be orthotropic and elastically-ideally plastic both in terms of compression and tension. The directions adopted for the analysis for the material data (Table 1) are presented in Figure 1. The assumptions of the constitutive model for wood in the elastic and plastic range are presented below.

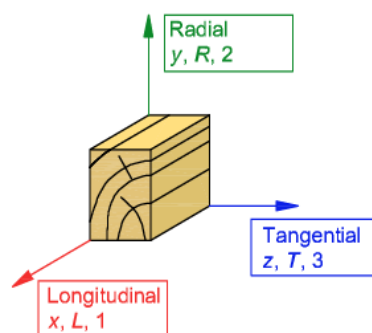


**Fig. 1.** Coordinate system adopted for numerical calculations (*own study*)

In terms of elasticity, a constitutive model based on the orthotropic characteristics of wood was adopted, written by the equation:

$$\{\varepsilon\} = [S] \cdot \{\sigma\} \quad (1)$$

where:

$\{\varepsilon\}$  – column vector of strains,

$[S]$  – an orthotropic compliance matrix with dimensions of  $6 \times 6$ , 1/Pa,

$\{\sigma\}$  – stress column vector, Pa.

The components of the equation can be represented as follows:

$$\{\varepsilon\} = \{\varepsilon_L \varepsilon_R \varepsilon_T \gamma_{LR} \gamma_{LT} \gamma_{RT}\}^T \quad (2)$$

$$[S] = \begin{bmatrix} 1/E_L & -\nu_{RL}/E_R & -\nu_{TL}/E_T & 0 & 0 & 0 \\ -\nu_{LR}/E_L & 1/E_R & -\nu_{TR}/E_T & 0 & 0 & 0 \\ -\nu_{LT}/E_L & -\nu_{RT}/E_R & 1/E_T & 0 & 0 & 0 \\ 0 & 0 & 0 & 1/G_{LR} & 0 & 0 \\ 0 & 0 & 0 & 0 & 1/G_{LT} & 0 \\ 0 & 0 & 0 & 0 & 0 & 1/G_{RT} \end{bmatrix} \quad (3)$$

$$\{\sigma\} = \{\sigma_L \sigma_R \sigma_T \tau_{LR} \tau_{LT} \tau_{RT}\}^T \quad (4)$$

where:

$\varepsilon_i$  – axial deformation,

$\gamma_{ij}$  – transverse deformation,

$E_i$  – axial modulus of elasticity (Young's modulus), Pa,

$\nu_{ij}$  – lateral deformation factor (Poisson's ratio),

$G_{ij}$  – shear modulus in three planes (Kirchhoff modulus), Pa,

$\sigma_i$  – normal stresses, Pa,

$\tau_{ij}$  – tangential stresses, Pa.

The yield point for wood as an orthotropic material was determined on the basis of the commonly used Hill plasticity criterion. It is a generalized version for anisotropic materials of the Huber-Mises hypothesis and is presented in equation (5)

$$f(\sigma, \sigma_y) = F(\sigma_{22} - \sigma_{33})^2 + G(\sigma_{33} - \sigma_{11})^2 + H(\sigma_{11} - \sigma_{22})^2 + 2L\sigma_{23}^2 + 2M\sigma_{31}^2 + 2N\sigma_{12}^2 - \sigma_y^2 = 0 \quad (5)$$

The coefficients from equation (5) were determined from formulas (6)-(17).

$$F = \frac{1}{2} \left( \frac{1}{R_{22}^2} + \frac{1}{R_{33}^2} - \frac{1}{R_{11}^2} \right) \quad (6)$$

$$G = \frac{1}{2} \left( \frac{1}{R_{33}^2} + \frac{1}{R_{11}^2} - \frac{1}{R_{22}^2} \right) \quad (7)$$

$$H = \frac{1}{2} \left( \frac{1}{R_{11}^2} + \frac{1}{R_{22}^2} - \frac{1}{R_{33}^2} \right) \quad (8)$$

$$L = \frac{3}{2} \left( \frac{1}{R_{23}^2} \right) \quad (9)$$

$$M = \frac{3}{2} \left( \frac{1}{R_{13}^2} \right) \quad (10)$$

$$N = \frac{3}{2} \left( \frac{1}{R_{12}^2} \right) \quad (11)$$

$$R_{11} = \frac{\sigma_{11}^y}{\sigma_0} \quad (12)$$

$$R_{22} = \frac{\sigma_{22}^y}{\sigma_0} \quad (13)$$

$$R_{33} = \frac{\sigma_{33}^y}{\sigma_0} \quad (14)$$

$$R_{12} = \sqrt{3} \frac{\sigma_{12}^y}{\sigma_0} \quad (15)$$

$$R_{23} = \sqrt{3} \frac{\sigma_{23}^y}{\sigma_0} \quad (16)$$

$$R_{13} = \sqrt{3} \frac{\sigma_{13}^y}{\sigma_0} \quad (17)$$

where:

$\sigma_y$  – yield point, Pa,

$\sigma_{ij}$  – stresses in the direction specified by indices, Pa,

$F, G, H, L, M, N$  – Hill plasticity coefficients,

$R_{ij}$  – Hill plasticity directional coefficients,

$\sigma_{ij}^y$  – strength in the direction specified by the indices, Pa,

$\sigma_0$  – comparative yield point, Pa.

**Composite bars.** The strength of fibrous composites is mainly influenced by the strength properties for the longitudinal axis, therefore the most frequently used constitutive model for composite materials is the isotropic, linear-elastic model. Therefore, this model was also adopted for the analysis. Calculations were made for four types of bar materials: basalt, glass, aramid and carbon. Material data was adopted on the basis of previous scientific studies (Table 1).

**Table 1.** Material data adopted in the numerical model (Rajczyk & Jończyk, 2018; Nowak et al., 2013; Yahyaiei-Moayyed & Taheri, 2011; Abu-Obaida et al., 2020; Hamzeh et al., 2020)

Characteristic	Unit	Timber	BFRP	GFRP	AFRP	CFRP
Young's modulus	MPa	$E_L = 9600$	$E = 56\,300$	$E = 52\,000$	$E = 51\,910$	$E = 147\,000$
		$E_R = E_T = 250$				
Tensile strength	MPa	$f = 19.2$	$f = 1474$	$f = 1100$	$f = 1400$	$f = 2800$
Kirchhoff modulus	MPa	$G_{LR} = G_{LT} = G_{RT} = 540$				
Poisson's ratio	–	$\nu_{LR} = \nu_{LT} = \nu_{RT} = 0.41$	$\nu = 0.3$	$\nu = 0.3$	$\nu = 0.34$	$\nu = 0.3$
Yield point	MPa	$\sigma_y = 38.15$				
		$\sigma_0 = 19.2$				
		$\sigma_{11y} = 19.2$				
		$\sigma_{22y} = \sigma_{33y} = 0.5$				
		$\sigma_{12y} = \sigma_{13y} = \sigma_{23y} = 3.5$				

## 1.2. Methods

In order to carry out a numerical analysis, a numerical model was prepared in Ansys 16.1. A beam subjected to four-point bending was adopted as a static diagram (Fig. 2a). Forces to the model and points of support were applied by means of steel flat bars, simulating the process of performing experimental tests. The articulated supports were made using the Remote Displacement function. Loads were declared with the Force command. The geometry was prepared in the Design Modeler module. Single lamellae were not analyzed, as the material data was assumed as for glued beams, in which the lamination effect was taken into account. The connection between the timber and the bars was set as Bonded. All contacts in the model used were assumed to be linear. The symmetry of the system was used for the calculations and the Symmetry Region command was used on two faces of the beams, finally assuming 1/4 of the full dimension (Fig. 2b). The size of the finite element type SOLID186 was assumed to be 1 cm. SOLID186 is a spatial element that easily adapts to difficult shapes, works well with irregular meshes, and is used to conduct nonlinear analyzes. It is a 20-node element with three node degrees of freedom (displacements in three directions).

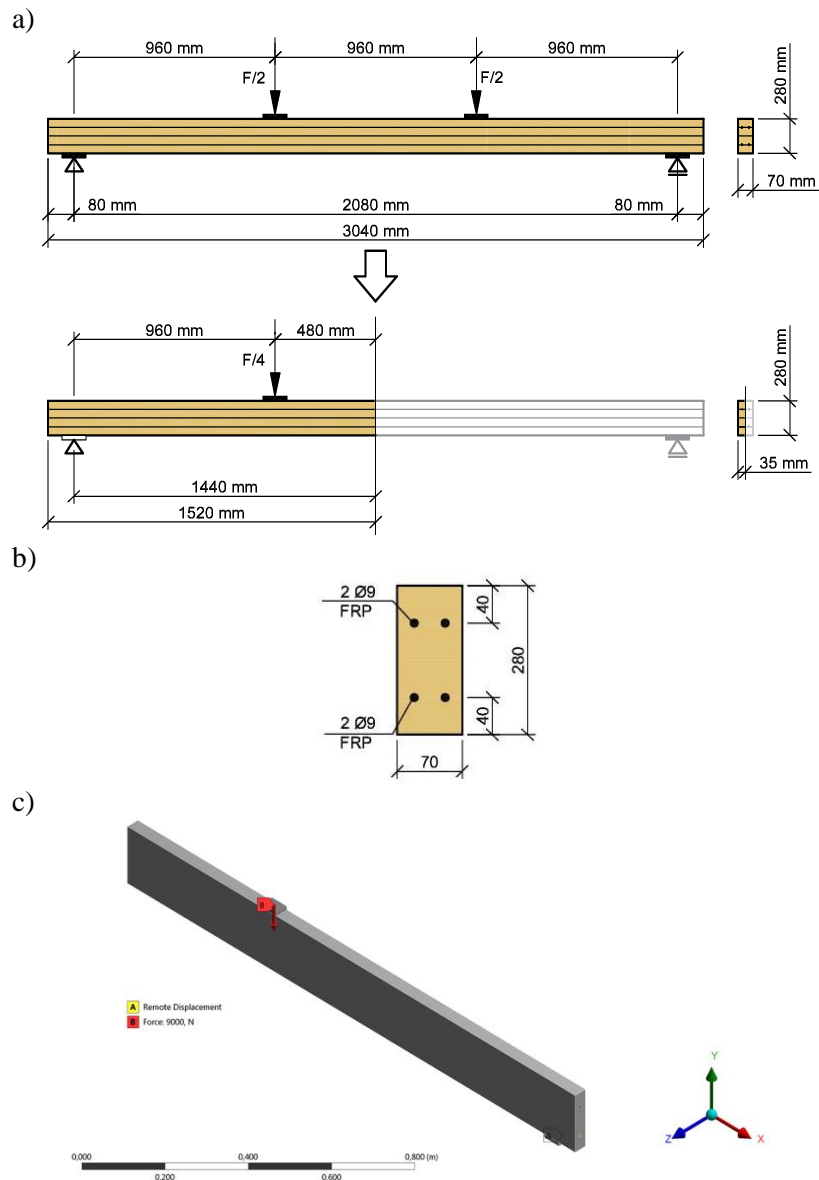


**Fig. 2.** Diagram of the tested beams: a) static diagram, b) cross section, c) numerical model (*own study*)

## 2. Results and discussion

Based on numerical calculations, the deflection-force diagram was presented for all reinforced beams and compared with the unreinforced beam (Fig. 3). Moreover, a diagram of normal stresses in the wooden cross-section of the reinforced beams and the witness beam is presented (Fig. 4).

All reinforced beams show greater stiffness compared to an unreinforced beam. A beam reinforced with CFRP carbon bars is characterized by a much higher stiffness among bars reinforced with bars. Beams reinforced with aramid, basalt and glass bars achieve a very similar stiffness, both in the elastic and plastic range. The distribution of normal stresses in reinforced beams is more favorable than in an unreinforced beam. Reinforced beams are characterized by a lower value of plastic stress, especially in the compressed zone. The most favorable distribution of normal stresses can be noticed in the beam reinforced with carbon bars, as the beam for the compared load value is the only one of the compared works in the elastic range.

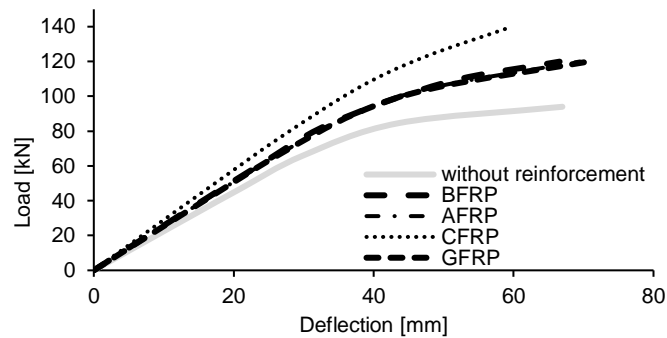


Fig. 3. Displacement-force plot for analyzed beams (*own study*)

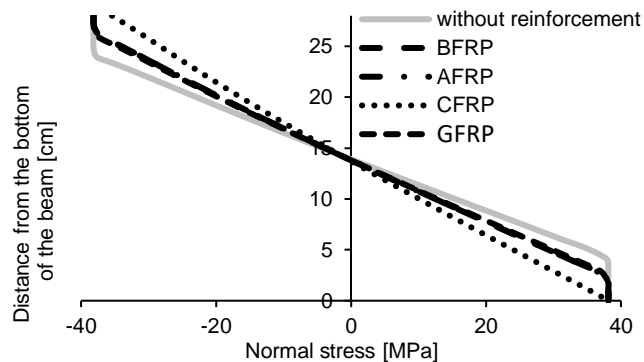


Fig. 4. The plot of normal stresses in timber for the analyzed beams (*own study*)

## Conclusions

The article presents the results of numerical calculations of wooden beams reinforced with composite bars made of various composite materials. It was assumed that the bars accepted for analysis were made with the use of basalt, aramid, glass and carbon fibers. During the analysis, the stiffness of the beams and the distribution of normal stresses in the wooden cross-section were compared.

The use of reinforcement in the form of composite bars has a positive effect on the static work of the beams. Stiffness and normal stress distribution in the wooden section of reinforced beams is more favorable than in the case of an unreinforced beam. The beams reinforced with CFRP carbon bars are characterized by the highest stiffness and the most favorable distribution of normal stresses. CFRP bars have the highest modulus of elasticity of all analyzed bars, therefore the improvement of the static work of beams reinforced with carbon bars is the most beneficial. When analyzing the distribution of normal stresses, it should be noted that the adoption of the elastic-plastic model for tensile stress is a simplification because, in fact, the tensile wood is destroyed by a brittle fracture.

### Acknowledgement

*The author is grateful for granting access to the computing infrastructure built in projects No. POIG.02.03.00-00-028/08 "PLATON – Science Services Platform" and No. POIG.02.03.00-00-110/13 "Deploying high-availability, critical services in Metropolitan Area Networks (MAN-HA)".*

### Bibliography

- Abu-Obaida, A., El-Maaddawy, T. & El-Ariss B. (2020) *Numerical simulation of double-sided concrete corbels internally-reinforced with GFRP bars*. Composites Part C: Open Access 2, 100040.
- Campilho, R.D.S.G., de Moura, M.F.S.F., Barreto, A.M.J.P., Morais, J.J.L. & Domingues, J.J.M.S. (2010) *Experimental and numerical evaluation of composite repairs on wood beams damaged by cross-graining*. Construction and Building Materials, 24, 531-537.
- Fossetti, M., Minafò, G. & Papia, M. (2015) *Flexural behaviour of glulam timber beams reinforced with FRP cords*. Construction and Building Materials, 95, 54-64.
- Hamzeh, L., Hassanein, A. & Galal, K. (2020) *Numerical study on the seismic response of GFRP and steel reinforced masonry shear walls with boundary elements*. Structures, 28, 1946-1964.
- Hollaway, L.C. (2010) *A review of the present and future utilisation of FRP composites in the civil infrastructure with reference to their important in-service properties*. Construction and Building Materials, 24, 2419-2445.
- Jasieńko, J. & Nowak, T. (2014) *Solid timber beams strengthened with steel plates – Experimental studies*, Construction and Building Materials, 63, 81-88.
- Jończyk, D. (2019) *A numerical analysis of different methods for strengthening beams made of glulam with CFRP fiber composites*, Zeszyty Naukowe Politechniki Częstochowskiej, Budownictwo, 25, 72-77.
- Kim, Y.J. & Harries, K.A. (2010) *Modeling of timber beams strengthened with various CFRP composites*, Engineering Structures, 32, 3225-3234.
- Lu, W., Ling, Z., Geng, Q., Liu, W., Yang, H. & Yue, K. (2015) *Study on flexural behaviour of glulam beams reinforced by Near Surface Mounted (NSM) CFRP laminates*. Construction and Building Materials, 91, 23-31.
- Nowak, T., Jasieńko, J. & Czepizak, D. (2013) *Experimental tests and numerical analysis of historic bent timber elements reinforced with CFRP strip*. Construction and Building Materials, 40, 197-206.
- PN-EN 338:2016-06 Drewno konstrukcyjne – Klasy wytrzymałości.
- Raftery, G.M. & Kelly, F. (2015) *Basalt FRP rods for reinforcement and repair of timber*. Composites: Part B, 70, 9-19.

Rajczyk, M. & Jończyk, D. (2018) *Badania belek z drewna klejonego warstwowo wzmocnionych prętami bazaltowo-epoksydowymi*. Zeszyty Naukowe Politechniki Częstochowskiej, Budownictwo 24, 298-304.

Yahyaeei-Moayyed, M. & Taheri, F. (2011) *Experimental and computational investigations into creep response of AFRP reinforced timber beams*. Composite Structures, 93, 616-628.

Yang, H., Liu, W., Lu, W., Zhu, S. & Geng, Q. (2016) *Flexural behavior of FRP and steel reinforced glulam beams: Experimental and theoretical evaluation*. Construction and Building Materials, 106, 550-563.